Control Study of Precision Giant Magnetostrictive Actuator Based on Active Disturbance Rejection Control Technology

Meng Wu
School of Information and Control Engineering, JiLin Institute of Chemical Technology, Jilin, China
Email: wu_meng@126.com

Hui Zheng
School of Computer Science, BeiHua University, Jilin, China
Email: Zhhui108@163.com

Zhongcheng Fan
School of Computer Science, BeiHua University, Jilin, China
Email: fanconnie@126.com

***Abstract*—Introduce the structure and working principle of precision giant magnetostrictive actuator and establish the actuator system object transfer function model so as to design a suitable active disturbance rejection controller (ADRC). According to the model analysis, regard the actuator system as a first-order inertia object with dead time to construct second-order ADRC, use MATLAB for parameter tuning and put the parameters into the controller to conduct simulation experiment on the actuator system objects. Simulation results show that the ADRC constructed has good control effect and strong anti-jamming ability and the parameters have strong robustness.**

***Index Terms*—giant magnetostrictive material, actuator, ADRC, parameter tuning, simulation**

I. INTRODUCTION

Giant magnetostrictive material (GMM) is a new functional material with magnetostrictive effect, able to realize electric-magnetic-mechanical energy conversion and provided with sensing and actuating functions. It has piezomagnetic effect (i.e., inverse magnetostrictive effect), that is, the material magnetization state changes in the external force, so it may be made into a variety of sensors. Actuation means that GMM changes in size in the magnetic field to convert magnetic energy into mechanical motion. Compared with traditional magnetostrictive materials and piezoelectric ceramics, GMM has better performance and is characterized by large strain capacity, fast response, large output force and easy control. Micro-displacement actuator designed and developed by using GMM has such advantages as high resolution (in micron), fast response (in microsecond), large output force, small size, low driving voltage, seamless transmission and simple control system, etc. Precision giant magnetostrictive actuator (GMA) is a device with actuation property developed by using GMM [1-13].

Precision giant magnetostrictive actuator makes use of the elongation/shortening response of GMM according to the size of the ambient magnetic field and the magnetic field control is usually achieved by the change in the drive coil current, so the performance of the drive system directly determines the actuation accuracy of the precision giant magnetostrictive actuator [14-15]. In order to improve the output accuracy of precision giant magnetostrictive actuator, domestic and foreign researchers use appropriate control algorithms in the closed-loop control of the drive system to expect that the size of the given value can be well reflected by the output value. Control algorithms should be generally selected to meet the needs of fast response, high precision and good stability of GMA. In addition, since precision giant magnetostrictive actuator is subject to a variety of interference factors from the environment in the application process, the output accuracy of GMA will be inevitably affected to some extent. The ADRC control algorithm is evolved from the nonlinear PID control algorithm. It not only inherits the advantages of the PID control algorithm such as simple, easy to implement and good robustness, but also overcomes the shortcomings such as unreasonable method to select errors, no error differential extraction method, undesirable mode of combination and the many side effects of integral feedback. It takes the effects of the system model as the internal disturbance and it together with the external disturbance of the system as the total disturbance so as to compensate the total disturbance, so it is a control algorithm with strong anti-interference ability and good

Corresponding author: Zhongcheng Fan.

doi:10.4304/jcp.7.11.2758-2764

robustness [16-20]. In combination with the driving principle and characteristics of GMA, this paper establishes a mathematical model of the GMA system and introduces ADRC in the process of automatic control to further improve the performance of the GMA control system.

II. WORKING PRINCIPLE OF GMA

Use domestic GMM rod (φ8×35) as the core to construct the precision giant magnetostrictive actuator as shown in Fig. 1. The actuator consists of giant magnetostrictive rod, preload spring, offset coil, drive coil and tighten screw, etc. The tighten screw and preload spring prestress the giant magnetostrictive rod to make its magnetic domain arranged as far as possible vertically along the axis in zero magnetic field in order to obtain the maximum magnetostriction in the magnetic field. The offset coil provides the bias magnetic field to make the work of giant magnetostrictive materials in its linear region, reduce the response insensitive zone and avoid frequency doubling. When a current passes through the drive coil, a driving magnetic field is generated and the giant magnetostrictive rod generates axial deformation under the action of the driving magnetic field to drive the output rod to move.

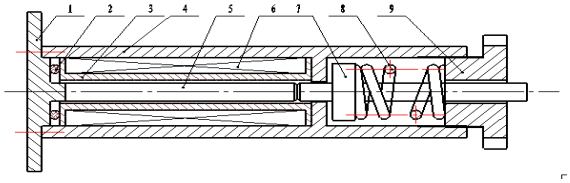

Figure 1. Theory Diagram of Giant Magnetostrictive Accurate-motion Actuator

1. Base; 2. Rubber loop; 3. Coil frame; 4. Outer coating; 5. GMM rod; 6. Offset coil and drive coil; 7. Output pole; 8. Preload spring; 9. Tighten screw

III. GMA MODELING

The GMA control system consists of GMA, drive power and controller, etc., as shown in Fig. 2. The actuator precision is affected by both the mechanical structure design and the performance of the drive power and drive system.

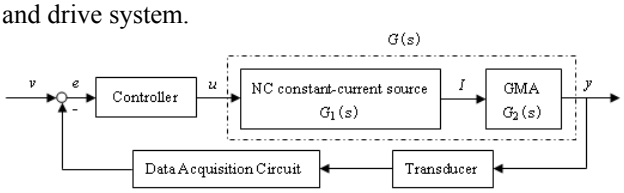

Figure 2. Block Diagram of GMA Control System

The displacement response of the GMA system includes the response characteristics of the drive power and GMA. Set the transfer function of the NC constant-current source is $G_1(s)$ and the transfer function of GMA is $G_2(s)$, then the transfer function of the control object $G(s)$ is:

$$G(s) = G_1(s) \cdot G_2(s) \quad (1)$$

According to the step response of the NC constant-current source, it may be approximately regarded as a first-order inertia object with dead time and its transfer function $G_1(s)$ is expressed as:

$$G_1(s) = \frac{K_1}{T_1 s + 1} e^{-\tau_1 s} \quad (2)$$

The analysis on the NC constant-current source characteristics shows that $T_1 = 0.03528s$, $\tau_1 = 0.00915s$ and $K_1 = \frac{dI}{du} = \frac{2A}{4000} = 0.0005A$. In the formula, du is power input digital variation; dI is power output current variation variation; du is from 0 to 4000 as drive power is from 0 to 2A.

Fig. 3 is the simulation curve of displacement step response when the digital input of the NC constant-current source is 4000.

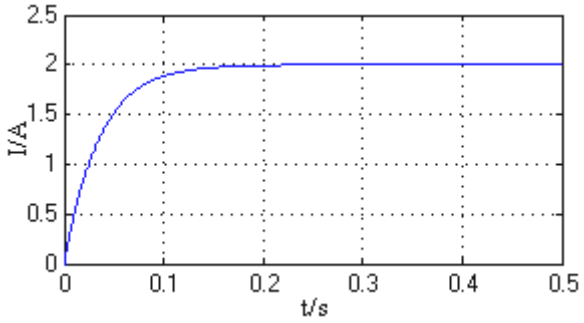

Figure 3. Step Response of NC Constant-current Source

In the work process, GMA always generates magnetostriction when one end is clamped or fixed and only moves along the axial direction [21-27]. So the actuator dynamic model as shown in Fig. 4 may be established.

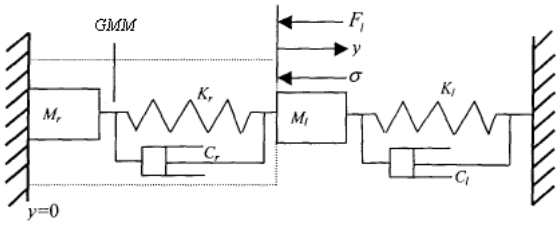

Figure 4. Actuator Dynamic Model

It is set that L, A_r, ρ and C_D respectively represents the length, cross-sectional area, mass density and internal damping coefficient of the GMM rod; K_r, C_r and M_r respectively represents the equivalent stiffness coefficient, equivalent damping coefficient and equivalent mass of the GMM rod; K_l C_l and M_l respectively represents the equivalent stiffness coefficient, equivalent damping coefficient and equivalent mass of the loads (including spring, ejector and mass loads); F, Y and σ_0 respectively represents the output force, displacement and prestress of the GMM rod and F_l represents the reaction force of the loads on the GMM rod.

Under the action of the driving magnetic field and pre-pressure, the GMA output displacement is derived as [28-29]:

$$y(s)=\frac{d_{33}HA_r/S^H}{(M_l+M_r)s^2+(C_l+C_r)s+(K_l+K_r)}$$
$$=\frac{\pi r^2 d_{33}N/LS^H}{(M_l+M_r)s^2+(C_l+C_r)s+(K_l+K_r)}I(s) \quad (3)$$
$$=\frac{K_2}{(M_l+M_r)s^2+(C_l+C_r)s+(K_l+K_r)}I(s)$$

In the formula, $H=NI/L$, $K_2=\pi r^2 d_{33}N/LS^H$, r represents the radius of the GMM rod, N represents the turns of the drive coil, S^H, d_{33} and H respectively represents compliance coefficient, piezomagnetic coefficient and magnetic field intensity when the magnetic field is a constant; $M_r=\rho LA_r/3$, $C_r=C_D A_r/L$, $K_r=\frac{A_r}{LS^H}$, L, A_r, ρ and C_D especively represents the length, cross-sectional area, mass density and internal damping coefficient of the GMM rod; K_r, C_r and M_r respectively represents the equivalent stiffness coefficient, equivalent damping coefficient and equivalent mass of the GMM rod; K_l, C_l and M_l respectively represents the equivalent stiffness coefficient, equivalent damping coefficient and equivalent mass of the load.

Transfer function of the GMA is:

$$G_2(s)=\frac{y(s)}{I(s)}=\frac{K_2}{(M_l+M_r)s^2+(C_l+C_r)s+(K_l+K_r)} \quad (4)$$

In actual calculation, the static gain K_2 can be derived using the following formula:

$$K_2=(K_l+K_r)\frac{dy}{dI} \quad (5)$$

In the formula, when the current variation is $dI=2A$, the displacement variation is $dy=20.12\mu m$.

Take the characteristic parameter values of the GMM rod as $\rho=9250\,kg/m^3$, $C_D=3\times10^6\,Ns/m^2$, $C_r=C_D A_r/L=4306\,Ns/m$, $C_l=1\times10^3\,Ns/m$, $M_r=\rho LA_r/3=0.005kg$, $M_l=0.5kg$, $S^H=1.5\times10^{-11}\,m^2/N$, $d_{33}=\partial\lambda/\partial H=1\times10^{-8}\,m/A$, $N=920$, $K_r=\frac{A_r}{LS^H}=9.6\times10^7\,N/m$ and $K_l=2\times10^6\,N/m$.

Put the parameters into the formulas (4) and (5), the transfer function of the GMA is derived as:

$$G_2(s)=\frac{1.94\times10^3}{s^2+1.05\times10^4 s+1.94\times10^8} \quad (6)$$

Fig. 5 is the simulation curve of unit step response of the GMA model. It can be seen from the figure that the overshoot of the result curve is large (about 27.78%), the rise time is very short (about 0.14ms) and the settling time is about 1ms.

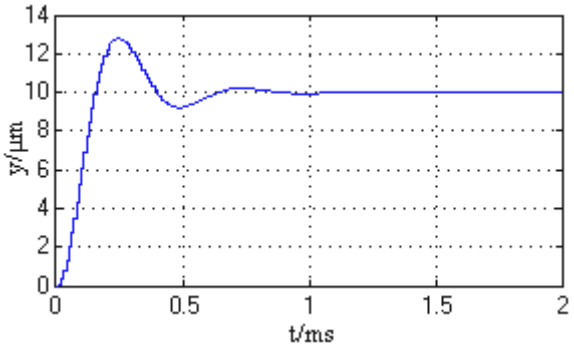

Figure 5. Step Response Curve of GMA

Put the formulas (2) and (4) into the formula (1), we get that

$$G(s)=\frac{K_1\cdot K_2}{(T_1s+1)\left[(M_l+M_r)s^2+(C_l+C_r)s+(K_l+K_r)\right]}e^{-\tau_1 s} \quad (7)$$
$$=\frac{0.0005\times1.94\times10^3}{(0.03528s+1)(s^2+1.05\times10^4 s+1.94\times10^8)}e^{-0.00915s}$$

Fig. 6 is the simulation curve of displacement step response when the GMA system digital input is 4000. The curve shows that the GMA system is a first-order inertia object with dead time and its response characteristics are mainly determined by the NC constant-current source. According to this feature, an inertia object with dead time may be used to represent the GMA system (see Formula (8)) and it is consistent with the response characteristics of the GMA system.

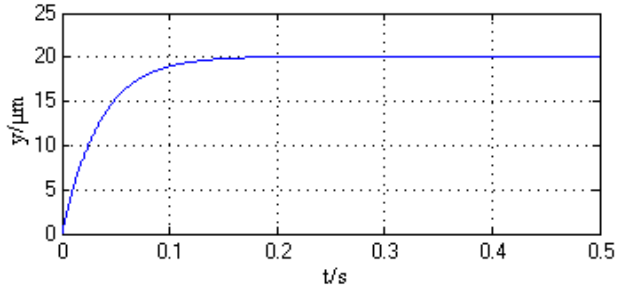

Figure 6. Displacement Step Response of GMA System

$$G(s)=\frac{y(s)}{u(s)}=\frac{0.005}{0.03528s+1}e^{-0.00915s} \quad (8)$$

IV. CONSTRUCTION OF GMA ADRC

A second-order ADRC is constructed in combination with the object properties and active disturbance rejection control technology, with structure as shown in Fig. 5. In the figure, TD is a differential tracker used to arrange the transient process V_1 and give the differential V_2; NLSEF is a nonlinear controller, which is nonlinear control strategy of the error between the transient process arranged and the object state variable and used to conduct nonlinear combination on the error e_1 and differential error e_2 and output control signal ; ESO is an extended state observer used to track the object displacement output y and estimate the object state variables of each order Z_1 and Z_2 and the real-time action of the object

total disturbance Z_3; G is the controlled object; b is the amplification factor of control input required to achieve active disturbance rejection control [16-20]. The corresponding equations are as follows:

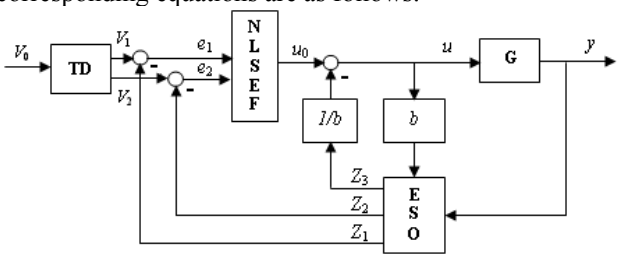

Figure 7. Structure of GMA ADRC

$$\text{TD}\begin{cases}\dot{V}_1 = V_2 \\ \dot{V}_2 = (4V_0/T_c^2)\ sign\ (T_t/2-t),\ \ t \le T_c \\ V_1 = V_0\ ,\qquad t > T_c\end{cases} \tag{9}$$

$$\text{ESO}\begin{cases}e_0 = Z_1 - y \\ \dot{Z}_1 = Z_2 - \beta_{01}e_0 \\ \dot{Z}_2 = Z_3 - \beta_{02}\,fal(e_0,\alpha_{01},\delta_0) + bu \\ \dot{Z}_3 = -\beta_{03}\,fal(e_0,\alpha_{02},\delta_0)\end{cases} \tag{10}$$

$$\text{NLSEF}\begin{cases}e_1 = V_1 - Z_1 \\ e_2 = V_2 - Z_2 \\ u = u_0 - Z_3/b = \beta_1\,fal(e_1,\alpha_1,\delta_1) \\ \qquad + \beta_2\,fal(e_2,\alpha_2,\delta_2) - Z_3/b\end{cases} \tag{11}$$

$$fal(e,\alpha,\delta) = \begin{cases}|e|^{\alpha}\,sign(e), & |e| > \delta \\ e/\delta^{1-\alpha}, & |e| \le \delta\end{cases} \quad \delta > 0 \tag{12}$$

In the formulas, V_0 is a given value; u is the control quantity; y is the object output; Z_1, Z_2 and Z_3 are the output of ESO, Z_1 and Z_2 can track the object state variables and Z_3 estimates the total action of the object disturbance; e_0 is the observation error of the state observer; T_c is the time of the transient process arranged; β_{01}, β_{02}, β_{03}, β_1, β_2 are correction factors. Function $fal(e,\alpha,\delta)$ is the output error correction rate, e is the error, α is the index and δ is the limit of error.

V. CONTROL OF GMA ADRC

A. PID Control Simulation of Actuator System

Fig. 8 shows the PID simulation curve of the object as shown in Formula (8). It can be seen from Fig. 8 that the overshoot of the PID control curve is about 53% and the settling time is relatively long at about 370ms.

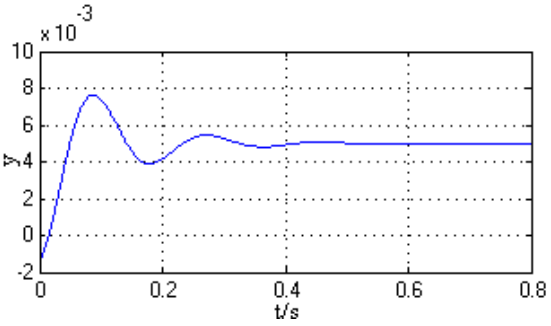

Figure 8. PID Simulation Curve of Actuator System

B. Actuator System Parameter Tuning and Simulation

It can be seen from the ADRC equations of the actuator that T_c, β_{01}, β_{02}, β_{03}, β_1, β_2, α_{01}, α_{02}, α_1, α_2, δ_0, δ_1, δ_2, b and h_0 are the parameters to be tuned in the equation, in which h_0 is the integration step for the discretization of the equation, i.e., sampling time.

The time constant and dead time of the actuator system objects are relatively small and it is difficult to determine the search range of the parameter tuning. Therefore, we can first select a regular first-order inertia object with dead time as the reference object, use MATLAB software to conduct ADRC parameter tuning and then use parameter transformation to transform into the actuator system ADRC parameters [30].

The reference object model is set as:

$$G_4(s) = \frac{K_4}{T_4 s + 1}e^{-\tau_4 s} = \frac{1}{20s+1}e^{-5s} \tag{13}$$

The parameters to be tuned of $G_3(s)$ are set as $\tilde{T}_c$, $\tilde{\beta}_{01}$, $\tilde{\beta}_{02}$, $\tilde{\beta}_{03}$, $\tilde{\beta}_1$, $\tilde{\beta}_2$, $\tilde{\alpha}_{01}$, $\tilde{\alpha}_{02}$, $\tilde{\alpha}_1$, $\tilde{\alpha}_2$, $\tilde{\delta}_0$, $\tilde{\delta}_1$, $\tilde{\delta}_2$, $\tilde{b}$ and $\tilde{h}_0$. The transient time is set as $\tilde{T}_c = 3.5(T_4 + \tau_4) = 87.5s$, and the MATLAB simulation software is used to tune the ADRC parameters of the reference object. Fig. 9 is the tuning diagram of the ADRC parameter $\tilde{\beta}_{03}$ of the reference object. Here, it is preset that $\tilde{\alpha}_{01} = 1$, $\tilde{\alpha}_{02} = 0.5$, $\tilde{\alpha}_1 = 0.2$, $\tilde{\alpha}_2 = 1$, $\tilde{\delta}_0 = 0.1$, $\tilde{\delta}_1 = 0.1$, $\tilde{\delta}_2 = 0.1$, $\tilde{b} = K_4/T_4 = 0.05$ and $\tilde{h}_0 = 1$. The assigned values of $\tilde{\beta}_{01}$, $\tilde{\beta}_{02}$, $\tilde{\beta}_1$ and $\tilde{\beta}_2$ are adjusted through software. It can be seen from Fig. 5.22 that $\tilde{\beta}_{03}$ changes within the interval of [0, 0.054] and there are 11 curves drawn in total. When $0 \le \tilde{\beta}_{03} < 0.005$, the curves of measurements and given values have large deviation; when $\tilde{\beta}_{03} > 0.052$, the measurement curve diverges; when $0.005 \le \tilde{\beta}_{03} \le 0.052$, the measurement curve is in good agreement with the given curve, i.e., the ADRC requirements can be met when $\tilde{\beta}_{03}$ selects any value within the range and the selection of parameters has good robustness. When $\tilde{\beta}_{03} = 0.02$, the ADRC effect is especially good. So it is selected that $\tilde{\beta}_{03} = 0.02$.

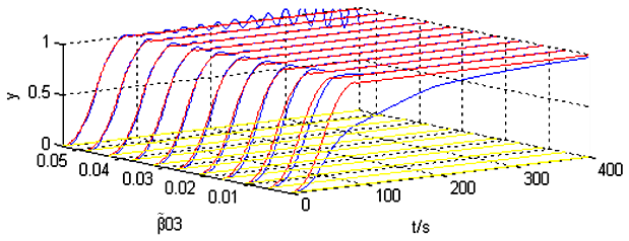

Figure 9. Tuning Diagram of ADRC Parameter $\tilde{\beta}_{03}$ of the Reference Object

After $\tilde{\beta}_{03}$ is selected, $\tilde{\beta}_{01}$, $\tilde{\beta}_{02}$, $\tilde{\beta}_1$ and $\tilde{\beta}_2$ may be tuned similarly. The parameters finally tuned are shown in Table 1.

TABLE I.

ADRC TUNED PARAMETERS OF THE REFERENCE OBJECT

$\tilde{T}_c$	$\tilde{\beta}_{01}$	$\tilde{\beta}_{02}$	$\tilde{\beta}_{03}$	$\tilde{\beta}_1$
87.5	0.3	0.3	0.02	1.2
$\tilde{\beta}_2$	$\tilde{\alpha}_{01}$	$\tilde{\alpha}_{02}$	$\tilde{\alpha}_1$	$\tilde{\alpha}_2$
30	1	0.5	0.2	1
$\tilde{\delta}_0$	$\tilde{\delta}_1$	$\tilde{\delta}_2$	$\tilde{b}$	$\tilde{h}_0$
0.1	0.1	0.1	0.05	1

Put the parameters into the ADRC equations and the results of control simulation on the reference object are shown in Fig. 10. It can be seen from the figure that the curve of measurements almost rises together with the curve of given values, indicating that the parameters tuned in this group are correct.

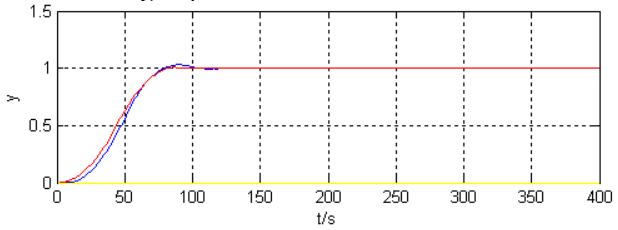

Figure 10. ADRC Simulation Curve of the Reference Object

Through calculation, the time constant ratio of the two objects is $m = T_3 / T_4 = 0.001764$ and the static magnification ratio is $n = K_3 / K_4 = 0.005$. The parameter tuning method is concluded according to parameter transformation, namely, the parameters (T_c, β_{01}, β_{02}, β_{03}, β_1, β_2, α_{01}, α_{02}, α_1, α_2, δ_0, δ_1, δ_2, b and h_0) of the actuator system $G_3(s)(T_3, K_3, \tau_3)$ are ($m\tilde{T}_c$, $\tilde{\beta}_{01}/m$, $\tilde{\beta}_{02}/m^2$, $\tilde{\beta}_{03}/m^3$, $\tilde{\beta}_1/n$, $m^{\tilde{\beta}_2}\tilde{\beta}_2/n$、 $\tilde{\alpha}_{01}$, $\tilde{\alpha}_{02}$, $\tilde{\alpha}_1$, $\tilde{\alpha}_2$, $\tilde{\delta}_0$, $\tilde{\delta}_1$, $\tilde{\delta}_2/m$, $n\tilde{b}/m^2$ and $m\tilde{h}_0$). By respectively putting the values of m and n into the corresponding relationship between the parameters, the ADRC parameters of the actuator system as shown in Table 2 may be obtained.

TABLE II.

PARAMETER VALUES OF ACTUATOR SYSTEM ADRC

T_c	β_{01}	β_{02}	β_{03}	β_1
0.15435	170	96410	3643630	240
β_2	α_{01}	α_{02}	α_1	α_2
10.584	1	0.5	0.2	1
δ_0	δ_1	δ_2	b	h_0
0.1	0.1	56.6893	80.342	0.001764

Put the parameters in Table Ⅱ into the ADRC equations and the results of control simulation on the actuator system are shown in Fig. 11. It can be seen from Fig. 11 that the measurements are in good consistency with the given values, the overshoot is very small and the control effect is the same as that of the reference object and much better than the traditional PID control, indicating the correctness and effectiveness to use the parameter transformation method for parameter tuning; the simulation program also develops the ADRC simulation curve as β_{03} of the actuator system object changes with $\tilde{\beta}_{03}$ of the reference object as shown in Fig. 12 which is consistent with the ADRC control trend of the reference object; when the parameters tuned change in a certain interval, the control effect will not be affected; in the practical application of ADRC after parameter tuning, for the objects with parameters (T, K, τ) changing within a certain range, the control effect is the same, which indicates that ADRC has strong robustness.

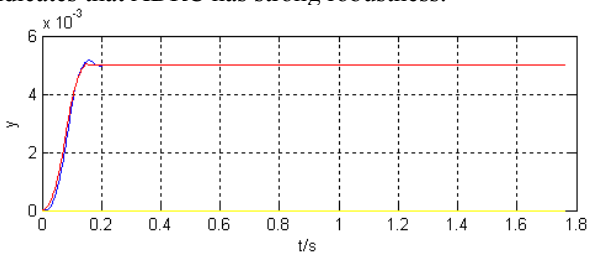

Figure 11. Simulation Curve of Actuator System ADRC

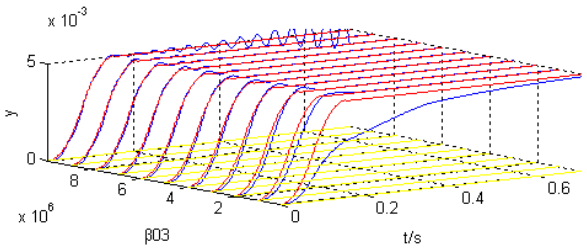

Figure 12. Diagram of Parameter β_{03} Turning of Actuator System ADRC

C. Anti-disturbance Analysis of Actuator System ADRC

ADRC is equipped with built-in anti-disturbance feedback loop, so it is relatively easy to realize the anti-disturbance properties better than other traditional controllers. System disturbance mainly includes feeding disturbance and load disturbance with feeding disturbance applied to the front and load disturbance directly applied onto the output of the control objects. Load disturbance is more difficult to control due to its

position of application. In the simulation experiment, sinusoidal disturbance signals with different amplitude(5%, 10%, 20% and 100% of the steady-state value respectively) are applied onto the output of the objects with software (see Fig. 13, 14, 15 and 16 for ADRC simulation curves).

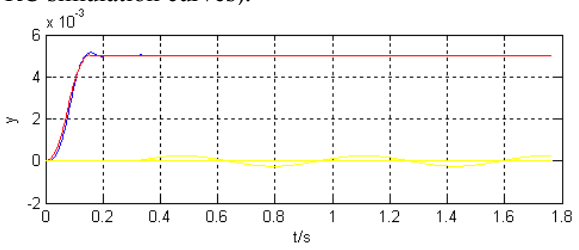

Figure 13. Simulation Curve of ADRC with Disturbance Amplitude at 5% of Steady-state Value

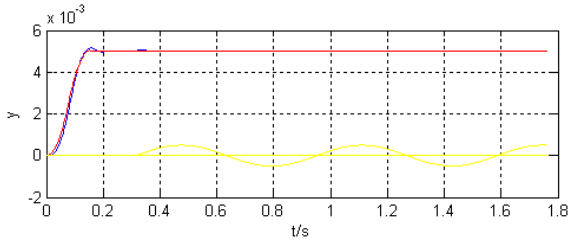

Figure 14. Simulation Curve of ADRC with Disturbance Amplitude at 10% of Steady-state Value

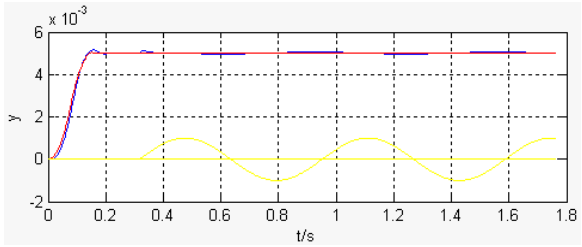

Figure 15. Simulation Curve of ADRC with Disturbance Amplitude at 20% of Steady-state Value

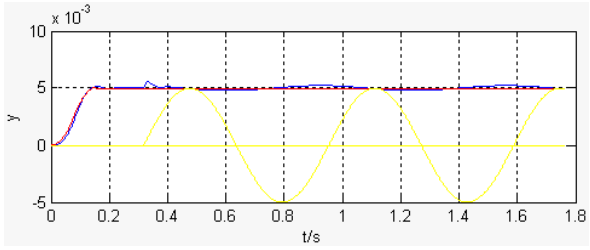

Figure 16. Simulation Curve of ADRC with Disturbance Amplitude at 100% of Steady-state Value

D. ADRC Program Design

The ADRC program flow is shown in Fig. 17. The amount of drive control may be given through arithmetic operations when only two port parameters, i.e., given target value and measured value, are provided to the controller software.

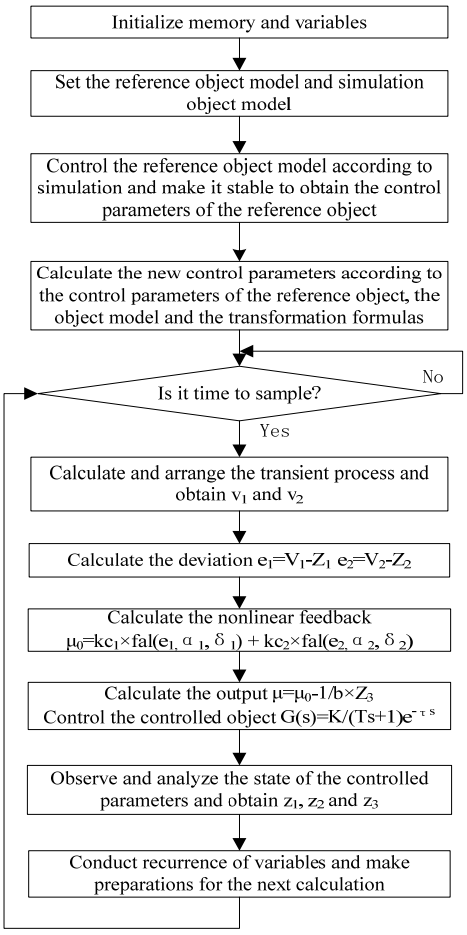

Figure 17. ADRC Program Flow Chart

VI. CONCLUSIONS

(1) The GMA system control object is a first-order inertia object with dead time;

(2) The ADRC simulation results show that the curves of measurements and given values are almost coincident and ADRC using tuning parameters has sound control effect;

(3) After parameter tuning, the system has a strong robustness, i.e., in a certain range, parameter variation has little effect on the stability of the system;

(4) It is observed from the four simulation curves that, when the disturbance amplitude is below 10% of the steady-state value, the measured curves vary slightly only when the disturbance just intervenes, but are immediately compensated by the ADRC loop, and the measurements remain consistent with the given values. With increasing disturbance amplitude, when the amplitude is higher than 20% of the steady-state value, the measured curves will fluctuate, but it still can be seen that the ADRC compensation effect is very obvious. By further parameter tuning, the inhibitory effect of ADRC on such disturbances will be made better.

REFERENCES

[1] Yu Peiqiong, Mei Deqing, Chen Zichen. "Design of a Micro-displacement Actuator Based on Giant Magnetostrictive Material," *Transactions of the Chinese*

Society for Agricultural Machinery, May, 2003, V34(N3), pp. 105-108.
[2] Judy J W. "Micro-electromechanical systems (MEMS)," *fabrication, design, and applications*[J], Smart Materials and Structures, 2001, 10, pp. 1115-1135.
[3] Jia Yuhui, Tan Jiubin. "Study on Micro-position Actuator System of Giant Magnetostrction Material," *Chinese Journal of Scientific Instrument*, 2000 , V21(N1), pp. 38-41.
[4] M. Knobel, K.R.Pirota, "Giant magnetoimpedance: concepts and recent progress," *Journal of magnetism and magnetic material*, 242-245(2002), pp. 33-40.
[5] Gabbert U, Tzou H S. "Smart structures and structure systems," *Proc of the IU TAM Symposium Held in Magdeburg*, *Germany Dordrecht Kluwer Academic Publishers*, September 2000, pp. 26-29.
[6] Babushka V, Donness O, Robert R. "Self-sensing actuators for precision structures," *Proceeding of the 1998 IEEE Aerospace Conference*, 1998,1(1), pp. 179-187.
[7] Eckhard Quandt, Alfred Ludwig. "Magnetostrictive actuation in Microsystems," *Sensors and Actuators*, 2000, 81, pp. 275-280.
[8] Yuan Huiqun, Li Dong, Sun Huagang. "Hysteretic Property of Rare Earth Giant Magnetostrictive Actuator," *Rare Earths*, 2007.6, 25, pp. 236-239.
[9] R.J.E. Smith, A.G.I. Jenner, A.J. Wilkinson, R.D. Greenough. "Magnetostrictive actuation performance under digital variable structure control," *Alloys and Compounds*, 1997, 258, pp. 101-106.
[10] Richard D. James. "New materials from theory: trends in the development of active materials," *Solids and Structures*, 2000, 37, pp. 239-250.
[11] F.Claeyssen, N.Lhermet, R.Le Letty, P.Bouchilloux. "Actuators, transducers and motors based on giant magnetostrictive materials," *Alloys and Compounds*, 1997, 258, pp. 61-73.
[12] Seok-Jun Moon, Chae-Wook Lim, Byung-Hyun Kim, Youngjin Park. "Structural vibration control using linear magnetostrictive actuators," *Sound and Vibration*, 2007, 302, pp. 875-891.
[13] Hartmut Janocha. "Application potential of magnetic field driven new actuators," *Sensors and Actuators*, 2001, 91, pp. 126-132.
[14] YANG Xing, JIA Zhenyuan, WU Dan, GUO Dongming, GUO Lisha. "Study on Driving Power of Giant Magnetostrictive Actuator Based on Power MOSFET," *PIEZOELECTRICS & ACOUSTOOPTICS*, 2001, V23(N1), pp. 33-36.
[15] FU Longzhu, DI Ruikun, XIANG Guofen. "The Study on Driving Power of Giant Magnetostrictive Actuator," *Mechanical & Electrical Engineering Magazine*, 2002, V19(N6), pp. 46-49.
[16] Han Jingqing. "From PID Technique to Active Disturbances Rejection Control Technique," *Control Engineering of China*, 2002.5, 9(3), pp. 13-18.
[17] Han Jingqing. "Nonlinear PID Controller," *ACTA Automatica Sinica*, 1994.7, 20(4), pp. 487-490.
[18] HAN Jingqing. "A New Type of Controller: NLPID," *CONTROL AND DECISION*, 1994, 9(6), pp. 401-407.
[19] XIA Yuanqing, HUANG Huanpao, HAN Jingqing. "ADRC control of uncertain systems with time-delay," *J.CENT.SOUTH UNIV.TECHNOL*, 2003, 34(4), pp. 383-385.
[20] HAN Jingqing. "Auto-disturbances-rejection Controller and It's Applications," *CONTROL AND DECISION*, 1998, 13(1), pp. 19-23.
[21] Lin Qing, Zhang Guoxian, He Qingwei, Yu Lan. "Modeling of Giant Magnetostrictive Actuators," *Mechatronics*, 2001.6, pp. 26-29.
[22] Xia Chunlin, Ding Fan, Lu Yongxiang. "Modeling of Giant Magnetostrictive Actuator," *China Mechanical Engineering*, 2000.11, 11(11), pp. 1288-1291.
[23] Song Renwang, Chen Linying. "Research of micro-displacement actuator modeling and simulation technology," *Transducer and Microsystem Technolgies*, 2007, 26(1), pp. 93-96.
[24] Viktor Berbyuk, Jayesh Sodhani. "Towards modelling and design of magnetostrictive electric generators," *Computers and Structures*, 2008, 86, pp. 307-313.
[25] Won-Je Park, Dae-Rak Son, Zin-Hyoung Lee. "Modeling of magnetostriction in grain aligned terfenol-D and preferred orientation change of terfenol-D dendrites," *Magnetism and Magnetic Materials*, 2002, 248, pp. 223-229.
[26] Wang Chuanli, Ding Fan, Zhang Kaijun. "The Study on Simulation of Dynamic Characteristic of Rare-Earth GMA," *Journal of System Simulation*, 2003.3, 15(3), pp. 379-381.
[27] Jia Zhenyuan, Yang Xing, Guo Dongming. "Study on Control Model of Giant Magnetostrictive Materials," *Piezoelectrics & Acoustooptics*, 2001.4, 23(2), pp. 164-166.
[28] Cao Shuying. "Dynamic Model with Hysteresis Nonlinearity and Control Technique for Giant Magnetostrictive Actuator," *Tianjin, Hebei University of Technology*, 2004.
[29] Weng Ling, Cao shuying, Wang Bowen, Fan Changzai. "Model and Simulation of Controlling System for Giant Magnetostrictive Actuator," *JOURNAL OF HEBEI UNIVERSITY OF TECHNOLOGY*, 2002.10, 31(5), pp. 27-30.
[30] ZHANG Xiaodong, TONG Shaowei. "Analyzing and Confirming the Parameters of ADRC with MATLAB Simulation," *CONTROL & MEASUREMENT*, 2006, 22(11-1), pp. 90-92.

Meng Wu born in Jilin, China in 1974, Ph.D. in Mechatronics Engineering, Mechanic Science and Engineering College, Jilin University, Changchun, China, 2009. Mainly engaged in electromechanical transmission and automation research.

He has been a lecturer in JiLin Institute of Chemical Technology since 1995. Until now, he has published six articles as the first author , which include:Design and Study on Power Supply for Giant Magnetostrictive Accurate-motion Actuator. Key Engineering Materials, 2009, 392-394: 787-792; New type of actuate-motion mechanism with giantmagnetostrictive and piezoelectric drive. Journal of HARRIN Institute of Technology, 2009, 41(1):149-151; A Study on Parameters Setting Methods for Active Disturbance Rejection Controller(ADRC). Transactions of Beijing Institute of Technology, 2009, 168(29):121-123. At present, he is mainly responsible for measuring and controlling work.

Dr. Meng Wu is a member of Academic Conference of China University Society on Manufacturing Automation.

Hui Zheng born in Jilin, China in 1972, postgraduate of Jilin University, associate professor of Beihua University, mainly engaged in database research.

Zhongcheng Fan born in Jilin, China in 1975, postgraduate of Changchun University of Technology, lecturer of Beihua University, mainly engaged in embedded systems research.